Thermally activated flux movement and critical transport current density in epitaxial $Bi_2Sr_2CaCu_2O_{8+\delta}$ films

P. Wagner, F. Hillmer, U. Frey, and H. Adrian
Technische Hochschule Darmstadt, Institut für Festkörperphysik, Hochschulstrasse 8, 64289 Darmstadt, Germany
(Received 6 December 1993)

In this article we report on thermally excited flux creep and the critical transport current density j_c in high-quality epitaxial $Bi_2Sr_2CaCu_2O_{8+\delta}$ thin films. Both dissipative mechanisms are governed by the highly anisotropic behavior of this compound which was investigated by means of the angular dependence of the magnetoresistivity ($\gamma \geq 150$). The activation energy U for thermally excited flux creep was evaluated with respect to temperature, magnetic field, and applied current density j. $U(T,B,j)$ is essentially increasing linearly with falling temperature, power-law dependent on the field ($U \propto B^{-\alpha}$ with $\alpha \approx 0.5$), and almost independent of current density for $j \leq 10^5$ A/cm^2. These experimental results are consistent with the concept of plastic flux creep. The critical current density exhibits high absolute values [$j_c(77\ \text{K}, B=0)=4\times10^5$ A/cm^2] and was measured for magnetic fields in the configuration $\mathbf{B}\|c$ up to 10 T and also with respect to various Θ angles between the c axis and field direction. The decrease of j_c with increasing B was found to be significantly reduced in comparison to single crystals and prior results on thin films. A further enhancement in the $j_c(B,T)$ behavior could not be achieved by chemical doping through partial substitution of copper by zinc.

I. INTRODUCTION

The bismuth cuprates form a stack of Josephson coupled CuO_2 layers with suppressed order parameter in the BiO doublelayers.[1,2] Therefore vortex lines decompose into pancake vortices located in the CuO_2 (single-, bi-, tri-) layers. Because of the small coupling energy between pancake vortices in adjacent CuO_2 layers they are nearly as easily thermally activated at higher temperatures ($t=T/T_c>0.5$) as individual pancake vortices. This thermally activated depinning gives rise to the significant broadening of resistive transitions in magnetic fields $\mathbf{B}\|c$ and to a strong decrease of the critical current density with increasing field. For $\mathbf{B}\perp c$ the compound behaves magnetically inert which was confirmed by the scaling behavior of the angular-dependent critical current density[3] and the magnetoresistivity.[4] The degradation of superconducting properties for $\mathbf{B}\|c$ limits the application range of wires and tapes at present to temperatures below $t=0.5$. Although the first epitaxial thin films prepared by laser ablation exceeded the critical current of bulk samples by two orders of magnitude, the detailed j_c data were, especially in external fields, not very encouraging in comparison to the critical currents that are easily obtained with $YBa_2Cu_3O_7$ thin films.[5] However, by a consequent optimization of the film quality j_c values can be achieved which are significantly higher than the values in the literature for all categories of samples, e.g., thin and thick films, polycrystalline or textured bulk material and single crystals. Meanwhile, the j_c values of liquid phase epitaxy prepared thick films are on the order of 10^6 A/cm^2 (Balestrino *et al.*) and in the range of 10^7 A/cm^2 for molecular beam epitaxy-prepared thin films (Bozovic *et al.*), in both cases in zero field at 4.2 K.[6,7] Therefore, one can assume that the improvement of the sample quality in thin-film preparation is accompanied by a decreasing number of defects to a density which is still suitable for an enhancement of j_c. In samples in the "clean limit," i.e., high-quality single crystals, the density of defects might be too low for a notable pinning effect, while in polycrystalline material j_c is predominantly limited by the presence of grain boundaries.

Despite large variances in j_c, measurements of the activation energy for thermally activated flux creep lead to very similar values $U(T\rightarrow0,B=1\ \text{T}) \approx 500-1800$ K regardless of the type of the sample or the evaluation method, indicating that the dominant dissipative mechanisms in these samples are of similar or related origin in the flux-creep regime. Additionally this indicates that there is no direct correlation between the activation energy and the critical current which is determined not only by the depth of pinning potentials, but also by their lateral extension, which is responsible for the pinning force density, and by the correlation volume of flux bundles. The following defect types have been suggested to act as pinning sites in Bi-2:2:1:2: oxygen vacancies as proposed by van der Beek and Kes,[8] twin boundaries in analogy to $YBa_2Cu_3O_7$ as suggested by Blatter,[9] grain boundaries in sintered material which were investigated by Müller, Nikolo, and Driver[10] and the typical screwed dislocations of $YBa_2Cu_3O_7$.[11] From the experimental point of view, at least the existence of oxygen vacancies in the CuO_2 planes is inevitable for thermodynamical reasons although their density can be reduced by appropriate annealing procedures. Screw dislocations could up to now neither be detected in *in situ* nor in *ex situ* prepared Bi-2:2:1:2 thin films[12,13] and also in $YBa_2Cu_3O_7$ films their influence on the pinning is unclear yet. A twinning within the *ab* plane seems to be an intrinsic defect at least for Bi-2:2:1:2 thin films, since there is a nonvanishing

difference between the a and the b axis of approximately 3×10^{-3} Å, caused by the incommensurate superstructure in the b direction. The lateral extension of coherent orientation within a and b axes was determined by plane view TEM.[14] It is of the order of at least 1500 Å, which is in agreement with results on films prepared by laser ablation.[15] For comparison in $YBa_2Cu_3O_7$ with its more pronounced a,b difference of ≈0.06 Å, the extension of these domains is in the range 500 Å.[16] To our present knowledge there is at least no evidence that ab twinning lowers the critical current, since the films discussed in this article exhibit ab twinning, while a j_c of 10^7 A/cm^2 at 4.2 K is reached reproducibly. Arbitrarily oriented grain boundaries, however, definitely induce a significant suppression of j_c in the case of thin films: As recently shown by Mayer *et al.* Bi-2:2:1:2 films deposited on $SrTiO_3$ grain-boundary substrates exhibit resistively shunted junction-like $I(V)$ curves and Josephson behavior in junctions placed over the grain boundaries.[17] The absence of these arbitrarily oriented boundaries for the films discussed here was confirmed by careful Φ scans with an angular resolution better than 0.2°.

II. EXPERIMENTAL

Thin films of Bi-2:2:1:2 have been prepared by an *in situ* sputtering method onto heated (100) $SrTiO_3$ substrates as described in detail in Ref. 12. For the films with zinc doping the composition of the target was modified to $Bi_{2.05}Sr_{2.00}Ca_{1.00}(Cu_{0.995}Zn_{0.005})_2O_{8+\delta}$, thus substituting 0.5% Cu by Zn with its completely filled $3d$ shell. Since the oxygen content of these films was not reduced by vacuum annealing for all samples under consideration, the resistive $T_c(\rho=0)$ was 84–88 K. $SrTiO_3$ was chosen because of the low lattice misfit and negligible interdiffusion. The high crystalline quality of the samples was confirmed by x-ray diffraction in Bragg-Brentano, Seeman-Bohlin, and four-circle geometry, by Rutherford backscattering, sputtered neutrals mass spectroscopy, scanning-electron and scanning-tunneling microscopy.[12] Especially the normal-state resistivity (280–450 $\mu\Omega$ cm at 300 K), the low minimum yield in channeling (23% for the Bi signal) and the narrow scattering in the c-axis orientation [full width at half maximum (FWHM) $(00\underline{10})=0.28-0.42°$] come very close to the values for high-quality single crystals. The patterning into a suitable eight-probe structure was accomplished by nondegrading photolithographic techniques.[18] This structure includes a 2mm$\times$200 μm stripline for resistive measurements and a 100 μm$\times$10 μm microbridge in order to perform the j_c measurements with low absolute currents to avoid heating effects, masking the intrinsic j_c values. For the same purpose annealed silver contacts were employed with a typical contact resistance below 10 mΩ. All voltages were measured in four-point geometry, while the dc currents were pulsed and reversed in order to eliminate the thermovoltages. The resistive data were taken at six different films in a thickness range from 3000 to 4200 Å while the current density was, if not mentioned explicitly, 100 A/cm^2, which is significantly below the threshold where the activation energy becomes dependent on the current itself (for comparison see Sec. III B).

III. RESULTS AND DISCUSSION

A. Anisotropy and angular-dependent properties

Regarding solely the chemical unit cell of Bi-2:2:1:2, it is very similar to $YBa_2Cu_3O_7$ concerning especially the mutual distance of the CuO_2 bilayers (3.1 and 3.8 Å, respectively) and the number and mobility of charge carriers in the CuO_2 planes [0.38–0.42 at 300 K per Cu atom with $\mu(100\text{ K})=19-22\ \mu$V] for both systems.[19] The pronounced anisotropy emerges from the distance between the bilayers in adjacent chemical unit cells which is 7.9 Å for $YBa_2Cu_3O_7$ and 12.3 Å for Bi-2:2:1:2, exceeding the coherence length $\xi_c(T=0)\approx2-3$ Å.[20] Dissipation arising from a magnetic field B tilted by an angle Θ versus the crystallographic c direction can be ascribed to the reduced field $B_{\text{red}}=B(\cos^2\Theta+1/\gamma^2\sin^2\Theta)^{1/2}$ in the sense of the scaling proposed by Blatter, Geshkenbein, and Larkin.[21] Defining the anisotropy parameter $\gamma(=\sqrt{m_c/m_{ab}})$ this way, the widely accepted values by Farrell *et al.* and by Raffy *et al.* were 55 as a lower bound and 29–36, respectively.[22,23] The crucial factor in these measurements however is the need for a narrow angular distribution of the c-axis orientation within the samples as all spread of this orientation lowers the derived γ values. Therefore, we emphasize that the intrinsic γ value for Bi-2:2:1:2 is considerably higher: Recent results by Steinmeyer *et al.* (magnetic torque at Bi-2:2:1:2 single crystals) gave a sample dependent γ between 140 and 900 at 77 K.[24] It is to note that $\gamma=140$ was obtained for a single crystal annealed in oxygen, while $\gamma=900$ was measured for a crystal with artificially reduced oxygen content by annealing in argon. This is a hint that the excess oxygen placed interstitially in the BiO double layers can act by charge transfer as a coupling between CuO_2 layers in adjacent chemical unit cells. The mechanical contraction, however, seems to be of minor influence for the resulting γ value as the measured c-axis difference between a heavily oxygen-overdoped film (with inductively measured T_c of 65–66 K) and a film with optimized oxygen content ($T_c=90$ K) was found to be less than 0.1, i.e, 30.78, and 30.85 Å, respectively.

In order to determine γ independently we made use of the scaling of the magnetoresistivity using a high-quality film [FWHM $(00\underline{10})=0.30°$ in Θ scan, $T_c^{\text{zero}}=88.0$ K achieved by optimizing the oxygen content, inductive transition width 1 K]. The magnetoresistivity measurements shown in Fig. 1(a) were performed at 85.10±0.01 K on a rotatable sample stage with Θ angles (angle between the c axis and field direction) of 0°, 30°, 60°, 75°, 84°, 87°, 89°, and 90°, while the current was always flowing perpendicular to the field direction. The relative resolution in the 90° position was better than 0.04°. All data points of Fig. 1(a) coalesce into one line by introducing the reduced field (field component perpendicular to the film's surface) $B|\cos\Theta|$, corresponding to $\gamma=\infty$, which is shown in Fig. 1(b). In the region of vanishing reduced field and resistivity [$\rho<1\mu\Omega$ cm, $B_{\text{red}}<1$ T in the inset of

Fig. 1(b)] we studied the coincidence of the data points for increasing γ parameters and a continuous improvement was still obtained for $\gamma > 150$ so that it was not possible to determine an upper bound of γ. From the fact that for $\mathbf{B}\|c$ the first occurrence of magnetoresistivity was observed at 40 mT, while for $\mathbf{B}\perp c$ no magnetoresistance could be detected even at $B = 6$ T one can conclude that γ is definitely above 150 which is significantly higher than the value of Farrell and in agreement with the data of Steinmeyer. It is to note that at the measurement temperature the magnetoresistance effects on the Pt temperature sensor are negligible.

Because of the divergence of ξ_c for $T \to T_c$ one should expect a coupling between CuO_2 bilayers in adjacent chemical unit cells for sufficiently high temperatures, resulting in notable deviations from the simple (two-dimensional) (2D) description which is still valid as close as 3 K below T_c. Angular-dependent measurements of the magnetoresistivity performed at 88.0, 89.0, 90.0, and 92 K for $B = 1$ T, see Fig. 2(a), can still be precisely described by the purely 2D-type scaling $\rho_{ab}(T, B = 1\ \text{T}, \Theta) = \rho_{ab}(T, B_{\text{red}} = 1\ \text{T} \cdot \cos\Theta, 0)$. The data points for magnetoresistivity in the orientation $\mathbf{B}\|c$ in Fig. 2(b) were parametrized by spline interpolation and taken for the (solid) fit lines in Fig. 2(a) which take completely into account the cusplike shape for $\Theta \to 90°$ without any evidence of rounding. This suggests that the conductivity above T_c is primarily based on 2D fluctuations and the assumed 3D temperature region is extremely narrow. In a recent article by Silva *et al.* it was demonstrated that there is indeed clear evidence for the 2D–3D transition by means of angular-dependent measurements of the depinning field slightly below T_c,[25] but there were no data for the scaling above T_c yet.

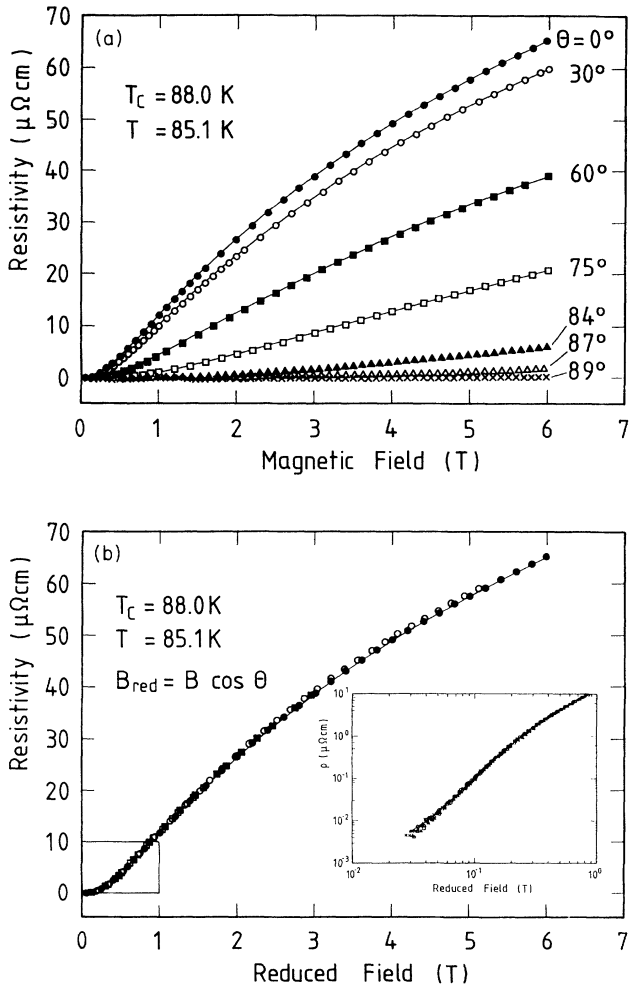

FIG. 1. Magnetoresistivity for a film with $T_c = 88.0$ at 85.10 K under various angles Θ between c axis and field orientation (a). In the case of $\Theta = 90°$ no magnetoresistivity is induced for $B = 6$ T. All curves coalesce with the $\Theta = 0°$ measurement by introducing the reduced field $B|\cos\Theta|$, corresponding to a quasi-2D behavior, while 150 is a lower bound for the γ parameter (b). The inset of (b) shows the region for reduced fields below 1 T on an enlarged scale.

B. Current dependence and temperature regime for thermally activated flux creep

In order to determine the temperature and current-density region where the model of thermally activated flux creep holds, for a detailed description see Ref. 26, the resistive transitions were measured for a film with $T_c^{\text{zero}} = 84$ K in a field of 1 T with currents from 1 μA to

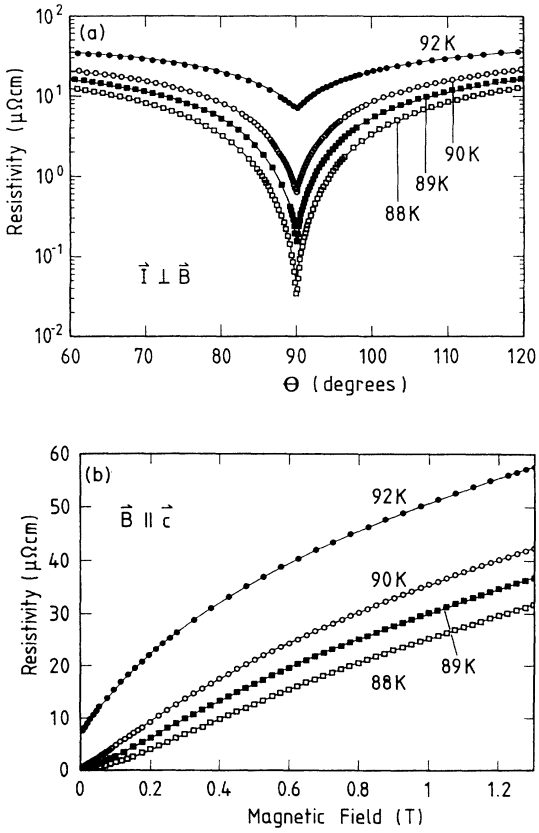

FIG. 2. Angular-dependent magnetoresistivity for $B = 1$ T at $T = 88.0$, 89.0, 90.0, and 92.0 K (a). The solid lines in (a) are fit functions based on the master curves for $\mathbf{B}\|c$ shown in (b). Note that the cusplike shape for $\Theta \to 90°$ remains even above T_c.

100 mA, corresponding to 1.25 A/cm^2 up to 1.25×10^5 A/cm^2. As can be seen from Fig. 3 the voltage vs 1000/T curves are shifted parallel and the local slopes do not depend on j although the current densities differ by five orders of magnitude. Therefore, it is not necessary to regard the limit $j\rightarrow0$ to evaluate the true activation energy, for which the slopes deliver a first approximation in the limit $T\rightarrow0$, as there is no hint for a drastically increasing or even divergent activation energy with decreasing current density. The temperature regime of linear Arrhenius plots in Fig. 3 ranges from approximately 80 down to 36 K where the resolution limit of the nanovoltmeter was reached in the case of the 100-mA measurement. Within this temperature interval the resistivity drops by six orders of magnitude from 10 to 10^{-5} $\mu\Omega$ cm. The broadening in the 100-mA curve (10^5 A/cm^2) in the low-temperature region is the first deviation from purely ohmic behavior and related to decreasing activation energy as heating effects have been strictly minimized. A notable decrease of the activation energy was observed in $YBa_2Cu_3O_7$ thin films as soon as the current density exceeded 10^3 A/cm^2. This was also reported by Zeldov *et al.* for Bi-2:2:1:2 thin films with a limit of 3×10^3 A/cm^2.[27] However the normal-state resistivity of Zeldov's sample is higher than that of our sample by a factor of 10 and the broadening in the external field is significantly more pronounced so that the threshold current densities cannot be compared directly.

In order to get an impression of the flux-creep temperature regime a suitable method is to examine the so-called "apparent activation energy" $f(t)=-d\ln\rho/dT^{-1}$, corresponding to the local slope of the Arrhenius plots. Figure 4(a) shows representatively $f(t)$ vs T of a film with $T_c^{zero}(B=0)=87$ K for $B=2$ T at temperatures close to T_c. The kink at 91 K, denoted by T^*, may be interpreted as a transition from the flux-flow mechanism to the creep dominated regime. T^* also corresponds to the temperature of the inflection point of the transition. Note that T^* does not shift by changing the field strength and at this temperature, with the evident change in the vortex dynamics, also measurements of the Hall effect exhibit the maximum amplitude of the negative Hall voltage. Although the onset of flux creep is commonly supposed to occur at temperatures where the resistivity is below 0.01 of its normal state value above T_c, we emphasize that at this temperature T^*, where $\rho\approx0.1\times\rho_n$, the apparent activation energy attains an equilibrium value. A lower temperature limit for flux creep in the vortex liquid regime cannot be derived from these data for small magnetic fields as the transition to the vortex-glass state is supposed to happen below 30 K, where the resistivity cannot be resolved exactly by means of a transport measurement. Arrhenius plots of resistive transitions in higher magnetic fields however, where the transitions can be studied to sufficiently low temperatures, exhibit notable changes from linear behavior. In order to enhance the resistivity resolution to 10^{-4} $\mu\Omega$ cm a transition in $B=6$ T was recorded with $j=10^4$ A/cm^2 allowing one to follow the resistive transition down to 30 K. The apparent activation energy $f(T)$, shown in Fig. 4(b), exhibits a clear increase below 30 K which indicates a beginning deviation from the creep mechanism and was related by Safar to a transition into the vortex-glass state.[28] As

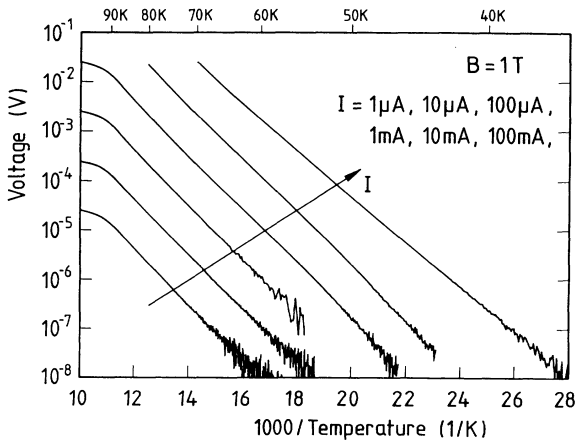

FIG. 3. Arrhenius plots of a resistive transition for $B=1$ T measured with six different currents ranging from 1μA to 100 mA. Only for the highest current, corresponding to 10^5 A/cm^2, the resistivity becomes current dependent and the local slope decreases at low temperatures.

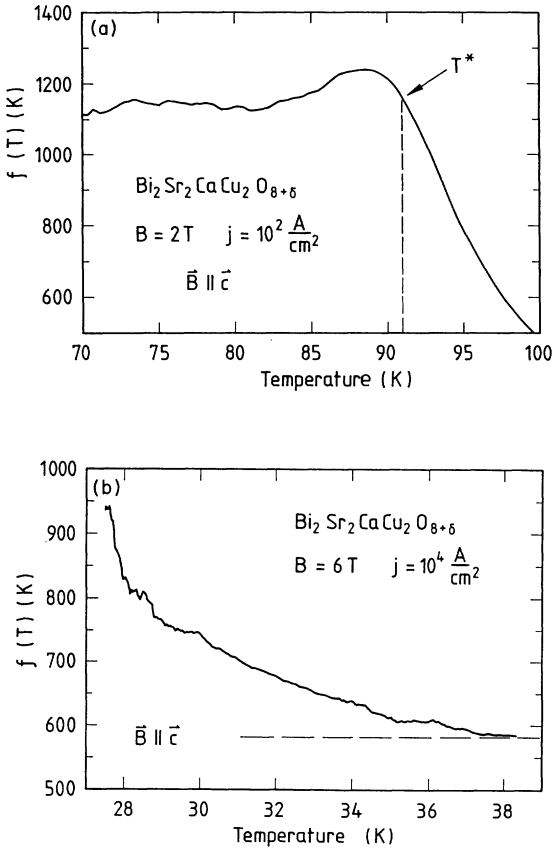

FIG. 4. Temperature dependence of the apparent activation energy $f(T)$ at $B=2$ T in the vicinity of T_c (a) and at low temperatures for $B=6$ T (b). Below the field-independent temperature T^*, $f(T)$ remains constant and undergoes a steady increase at 30 K which can be related to a transition from the vortex-liquid to vortex-glass state (Ref. 28).

the data of Safar were taken for a single crystal with especially weak pinning, this transition leads to an abrupt divergence in $f(T)$. For the thin film with its significantly higher value for $f(T)$ also above the transition temperature the transition seems to be smeared and shifted to higher temperatures. However from the existence of this transition we suppose that also in the comparatively strong pinning films the flux-line dynamics are governed by a collective behavior rather than by core pinning of individual flux lines where this kind of transition should not be directly observable.

C. Evaluation of $U(T,B)$

In Figs. 5(a)–5(d) the resistive transitions are shown as ρ vs T plots and as Arrhenius plots ($\log_{10}\rho$ vs $1/T$) for the magnetic fields 0, $\frac{1}{16}$, $\frac{1}{8}$, $\frac{1}{4}$, $\frac{1}{2}$, and 1 T, and 0, 1, 2, 4, 6, 8, and 10 T, respectively. It is obvious that the Arrhenius plots in Figs. 5(b) and 5(d) form almost straight lines for all fields. For the evaluation of the true activation energy $U(T,B)$ it is necessary to adopt certain models or at least reasonable assumptions: The local slope of the Arrhenius plots does only directly correspond to the activation energy if U is either temperature independent (which is physically unreasonable) or increasing strictly linear with decreasing temperature, i.e., if $U(t)=U_0(1-t)$ with $t=T/T_c$, then f is independent of temperature and $f=U_0$. Taking into account the model discussed by Palstra *et al.*,[26] $U(t)$ should be related to the condensation energy as $U(t)=U_0H_c^2(t)\xi^n(t)$. The exponent $n(=1,2,3)$ depends on the dimensionality of the system and $H_c(t)$ and $\xi(t)$ can be expressed by the parabolic approximations $H_c(t)\propto 1-t^2$ and $\xi^2(t)=(1+t^2)/(1-t^2)$. Provided that this model holds for the description of experimental data, $f(t)$ has independently of n a pronounced curvature for $0.5<t<1$ (this is the experimentally accessible region) and U_0 and $U(t)$ can be extrapolated by compensation factors (coming close to unity for $t<0.5$) which were calculated by Seng *et al.*[29] Nevertheless it is not possible to obtain convincing fits to the straight Arrhenius plots by these attempts (with any integer exponent n, while $n=1$ delivers qualitatively the best results) and the reason may be that the idea of core pinning standing behind this model does not apply for $Bi_2Sr_2CaCu_2O_{8+\delta}$ and other two-dimensional compounds, while a model based on weak collective pinning is probably more appropriate. Thus $U(B,T)$ will be evaluated directly from the $\rho(B,T)$ data independently of a peculiar model assuming only that $U(T_c)=0$. To our present knowledge, three inversion procedures have been proposed in the literature.

(i) Palstra *et al.* suggest to solve the basic relation $\rho(T)\propto\exp[-U(T)/k_BT]$ for $U(T)$, for simplicity the explicit field dependence is omitted here.[30] As starting point of the evaluation we use the expression

$$\rho(T,B)=\rho(T^*,B)\exp[-U(T,B)/k_BT]\ ,$$

resulting in

$$U(T,B)=k_BT[\ln\rho(T^*,B)-\ln\rho(T,B)]\ .$$

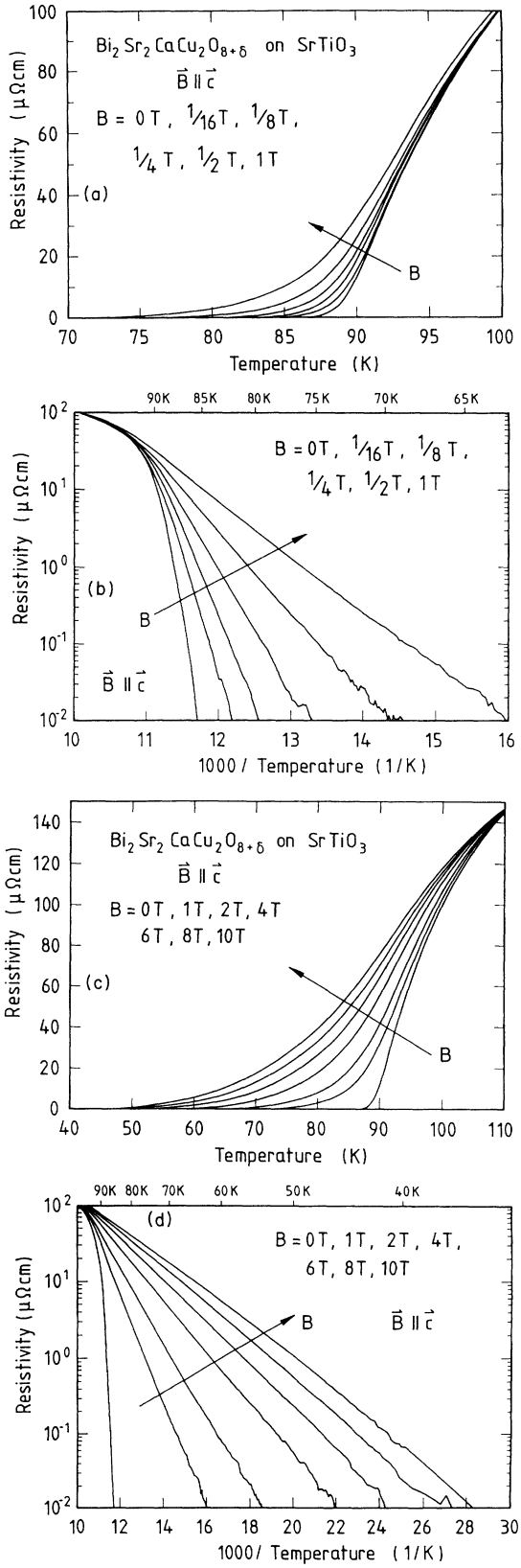

FIG. 5. Resistive transition of an epitaxial, pure Bi-2:2:1:2 thin film in different magnetic fields $\mathbf{B}\|c$. (a) and (b) show the resistivity data for small fields ($B=0$, $\frac{1}{16}$, $\frac{1}{8}$, $\frac{1}{4}$, $\frac{1}{2}$, 1 T) on a linear scale and as Arrhenius plots. (c) and (d) show the corresponding data for $B=0$, 1, 2, 4, 6, 8, 10 T.

The exponential prefactor $\rho(T^*,B)$ corresponds to the resistivity at the field B and the temperature T^*, denoting the temperature at the inflection points of the transitions (mean field T_c) which is field independent at least for 0.1 T $< B <$ 10 T and below of which $f(T)$ remains almost constant, see Fig. 4(b). In the case of the sample of Fig. 5, $T^*(B)$ is 91.5 K±0.5 K, while T_c^{zero} $(B=0)=87.0$ K. By this choice of ρ_0, the activation energy vanishes at the mean field T_c and $\rho(T^*,B)$ has a physical meaning. Note that the resulting $U(T,B)$ depends on the particular choice of ρ_0 only to a minor part as it represents only an additive constant without influence on the variation with temperature. Therefore it does especially not alter the result when a $1/T$ dependence of the prefactor is taken into account as suggested in Ref. 26.

(ii) The procedure prosed by Chui and Ma[31] is based on the integration of $f(T)=-d\ln\rho/dT^{-1}=T^2d(U/T)/dT$, which can be obtained by a numerical derivation of the $\rho(B,T)$ data in Arrhenius form. Numerical integration results in $U(T)=T\int_{T_c}^{T} f(T)/T^2dT$, which also allows the activation energy to become zero for $T\rightarrow T_c$. The methods (i) and (ii) can be shown to be analytically equivalent.

(iii) The inversion scheme by Hagen and Griessen is not directly applicable to the transport measurements, but it allows to extract a whole spectral distribution of pinning potentials with different activation energies from magnetic relaxation data.[32] The complication of a distribution of activation energies will not be taken into account in this article.

In Fig. 6 the activation energies were derived by method (i) with the calibration $U(T^*=92\text{ K})=0$ for all magnetic fields. $U(T,B)$ is in a first and rather good approximation indeed increasing linearly with falling temperature in a very similar way as published by Kucera *et al.*[33] The absolute $U(T,B)$ values are almost equal too, although there are significant differences in T_c, j_c and most pronounced in the normal-state resistivities. The measurement at 10 T exhibits a slight tendency to an increase $U\propto(1-t)^{\alpha}$ with α higher than one. Therefore, ignoring the effect of a vortex-glass transition which increases the activation energy drastically below 30 K, the average-slope data are in fact an approximation of $U(T,B)$ extrapolated from high temperatures to $T=0$. The $\log_{10}U_0$ vs $\log_{10}B$ plot in Fig. 7 shows these extrapolated activation energies of four different samples and fields between $\frac{1}{16}$ and 10 T. The straight lines are least-square fits of the relation $U\propto B^{-\alpha}$ to the data with sample-dependent exponents $0.52\leq\alpha\leq0.54$ coming close to the value of $\alpha=0.5$. Because of the linear U vs T relation this power law holds independently of temperature. In Fig. 7 it can be seen directly that the activation energies for the zinc-doped films are of the same absolute value as for undoped samples and there is no hint for an increase of U by the chemical doping, at least at a concentration of 0.5% Zn, which was found to be very pinning effective in thin $YBa_2Cu_2O_7$ films.[34]

A theoretical attempt predicting exactly the $U\propto(1-t)/\sqrt{B}$ behavior is the model of plastic flux creep ascribing the dissipation to the plastic shear of dislocations in a weakly pinned vortex liquid by Geshken-

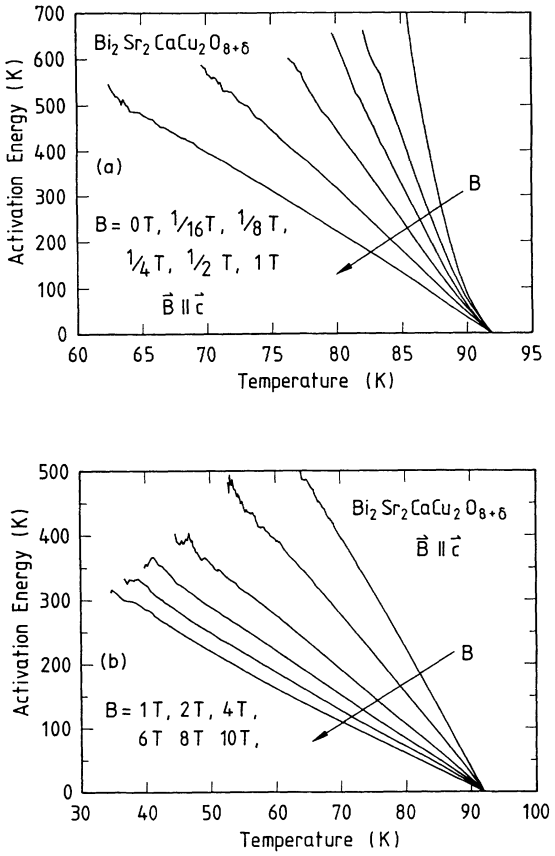

FIG. 6. Temperature dependence of the activation energy $U(B,T)$ for fields below 1 T (a) and for fields up to 10 T (b), evaluated by the inversion procedure described in the text. Through the linear behavior in T, the peculiar field dependence of U is independent of temperature.

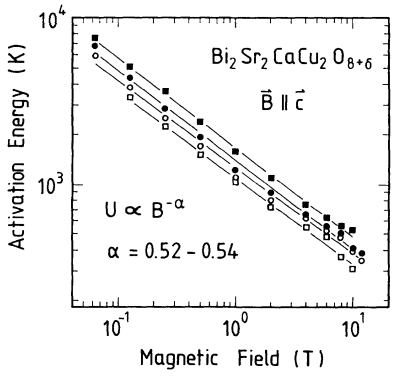

FIG. 7. Activation energies for four different Bi-2:2:1:2 films in fields between 1/16 and 10 T, derived from the slope of the Arrhenius plots in the low resistance regime (10^{-2}–$1\mu\Omega$ cm). Samples indicated with □ and ■ are pure Bi-2:2:1:2, while the symbols ○ and ● stand for data derived from films doped with 0.5% Zn. The zinc doping does not result in an enhancement of $U(B)$. The lines represent least-square fits to the data with slopes close to $\frac{1}{2}$.

bein and co-workers.[35,36] In this model the activation barrier corresponds to the free-energy increase caused by the formation of a double kink in a (continuous) flux line which is the free energy of two vortex segments with a typical length of the vortex lattice constant a ($\propto 1/\sqrt{B}$), lying in the ab plane when the field is in c direction. The qualitative expression for this energy is $U_{Pl} \approx \sqrt{m_{ab}/m_c}\Phi_0^2 a/8\pi^2\lambda_c^2$, which brings about the characteristic field and temperature dependences. Making use of anisotropic Ginzburg-Landau theory, as performed in the article by Kucera *et al.*,[33] the quantitative result for $B=1$ T with a γ parameter of 150 is $U_0=1450$ K, which agrees with the experimental data surprisingly well (1200–1700 K). However, we want to point out that it is at present not definitely clear why this theory seems to apply almost perfectly as the theory is based on the concept of a (anisotropic) three-dimensional system but not on a two-dimensional compound with clear evidence for the formation of decoupled pancake vortices. Nevertheless, the plastic flux creep seems to be the mechanism of dissipation that is suitable for the proper qualitative description of a large variety of high-temperature superconducting materials except $YBa_2Cu_3O_7$, which exhibits curved Arrhenius plots.[26] Approximately straight Arrhenius plots have been also found in $Bi_2Sr_2CaCu_2O_{8+\delta}$ single crystals,[26] in polycrystalline $Bi_2Sr_2CaCu_2O_{8+\delta}$ thin films with random ab orientation,[37] in $Bi_2Sr_2Ca_2Cu_3O_{10+\delta}$ thin films[38] with T_c equal to the Bi-2:2:1:2 film discussed here, in high-quality YBCO/PrBCO superlattices,[39,40] in ultrathin $YBa_2Cu_3O_7$ films,[41] in films and single crystals of the thallium compounds[42] and in polycrystalline samples of $Pb_2Sr_2Y_{0.5}Ca_{0.5}Cu_3O_8$.[43] Thus this feature of the Arrhenius plots is common to all systems with either intrinsic or artificially tailored two-dimensional behavior. However, we do not want to ignore that the scaling U vs B does not deliver a power law with exponent 0.5 for all cases, as this dependence seems to be very sensitive to the actual sample quality. The formation of vortex kinks is more probable than the collective motion of ensembles of vortex lines as the line tension in these compounds is strongly reduced. Due to the weak correlations along the pancake stack the addition of the zinc atoms can therefore not hinder the formation of these kinks and this lack of pinning by pointlike defects was also found in a recent article by vom Hedt, Westerholt, and Bach by zinc doping of Bi-2:2:1:2 single crystals.[44]

D. Critical current density

Figure 8 shows the temperature dependence of the critical current density j_c in zero field measured with a 1-μV criterion along the 100-μm microstrip for a pure Bi-2:2:1:2 film and a film doped with 0.5% Zn, which do not exhibit significant differences. In order to get an impression of the criterion dependence, the inset of Fig. 8 shows $j_c(T)$ as determined at the 2-mm-long stripline with the criteria 1 and 10 μV: At 77 K the critical current densities are 3×10^5 and 4×10^5 A/cm^2, respectively, at 70 K the corresponding values are 8×10^5 and 1×10^6 A/cm^2. Therefore, at least below 80 K, there is no striking influence of the criterion on the measured j_c. It is

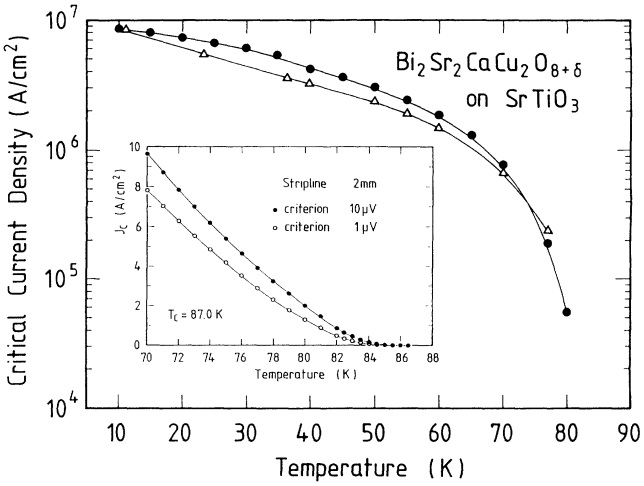

FIG. 8. Critical current density in zero field for an epitaxial, pure Bi-2:2:1:2 film (−△−) and a film doped with 0.5% Zn (−●−), both with a criterion of 1 μV for a 100-μm microstrip. The insert shows (on a linear scale) $j_c(T)$ of the undoped film for two different voltage criteria (1 μV and 10 μV) in case of the 2-mm stripline.

noteworthy that below 80 K the increase of the zero field $j_c(T)$ is almost strictly linear with falling temperature at a rate of 10^5 A/(cm^2 K). This linearity was already measured by Schmitt and related to the total annealing time of these laser-ablated films.[45] Thus the critical current density is enhanced and the originally negative curvature of $j_c(T)$ shifted to a linear behavior for prolonged thermal annealing below the melting point in pure oxygen as it is also performed for the sputtered Bi-2:2:1:2 films described here. This annealing process cannot be supposed to produce pinning-active defects by itself, the supposed defects are probably created already during the growth process. We suggest that healing effects in the crystal lattice are related to the filling of the oxygen sites lowering the density of the pair-breaking oxygen vacancies. This linear increase in zero field j_c is significantly different from the behavior in single crystals as measured by Metlushko *et al.*:[46] The pinning in high-quality single crystals is, due to the supposed lack of suitable pinning sites/defects so weak, that below 20 K an abrupt j_c increase by two orders of magnitude is observed which is related to a crossover from independently moving pancake vortices (in the vortex liquid regime) to a coupling between the pancakes in adjacent layers as soon as the coupling energy exceeds the thermal energy. In the strongly pinning-active films there is no clear evidence for the existence of such a transition, as j_c at 70 K is as high as for single crystals at 4.2 K.

The decay of j_c with increasing external field $\mathbf{B}\|c$ is shown in Fig. 9 for fields up to 9 T, measured at the 10-μm-wide microstrip with a 1-μV criterion. The angular dependence of $j_c(T,B,\Theta)$ was found to be in complete agreement with the former results of Schmitt concerning the 2D-type scaling

$$j_c(T,B,\Theta)=j_c(T,B_{\mathrm{red}}=B\cdot\cos\Theta,0)$$

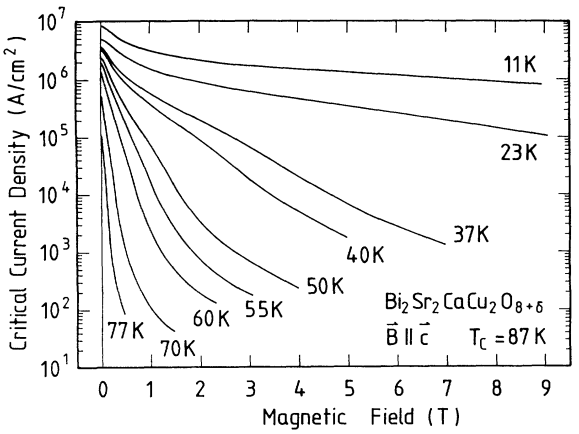

FIG. 9. Critical current density at fixed temperatures for fields $\mathbf{B}\|c$ up to 9 T. Due to the high density of data points they are represented as solid lines. The established values for epitaxial Bi-2:2:1:2 films prepared by laser ablation are exceeded by two decades in the intermediate temperature range (Ref. 5).

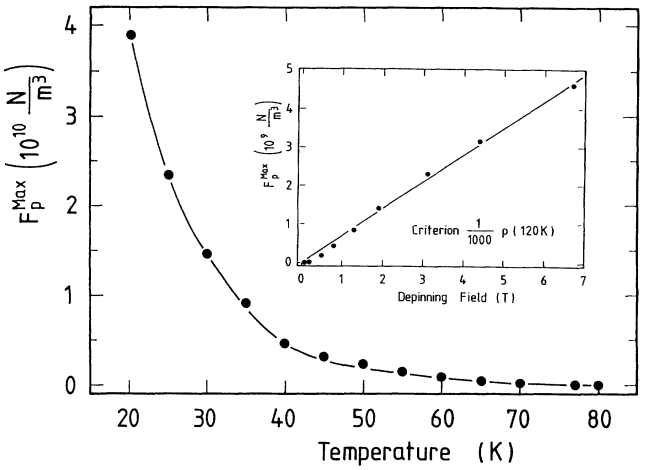

FIG. 10. Maximum pinning force density F_p^{max} for Bi-2:2:1:2 versus temperature. The increase is proportional to $(1-T/T_c)^4$, while F_p^{Max} depends approximately linear on the depinning field for temperatures above 40 K. The depinning field was defined by a 0.1% criterion of the normal-state resistivity.

(Ref. 3) and angular-dependent j_c data of the films discussed in this article have been recently published in Ref. 47. Besides the increased zero-field critical current densities of the sputtered films compared to the laser-ablated films, in the average by a factor of 4, the most remarkable improvement is the drastically reduced decline with increasing field. The resulting differences, dependent on temperature and field, are up to two or even three orders of magnitude which is especially apparent in an intermediate temperature range in higher magnetic fields.[5] For temperatures below 30 K, the j_c decay is additionally reduced, so that a 11 K even in a field of 9 T j_c is still 10^6 A/cm^2.

At present the $j_c(T,B)$ relation can only be described in a phenomenological way: Fig. 10 shows the maximum pinning force density $F_p^{max}(T)=[j_c(T,B)\cdot B]^{max}$ versus temperature for a Zn-doped film, behaving completely equivalently to the pure Bi-2:2:1:2 samples. For temperatures below 40 K, i.e., in the supposed vortex-glass state, the increase of F_p^{max} is in very good approximation proportional to $(1-T/T_c)^4$. A comparison of $F_p^{max}(T)$ with the depinning field $B_{dep}(T)$, defined here as $\rho[B_{dep}(T),T]=10^{-3}\rho_n$ (120 K), in the regime of the weakly pinned vortex liquid above 40 K reveals $F_p^{max}(T)\propto B_{dep}(T)$ as shown in the inset of Fig. 10. This behavior is clearly different from the relation $F_p^{max}(T)\propto B_{dep}(T)^{\alpha}$ with α between 1.6 and 2.2, which was determined by Speckmann *et al.* for epitaxial $YBa_2Cu_3O_7$ thin films,[48] but it is in full agreement with the data for epitaxial Bi-2:2:2:3 films by Yamasaki *et al.*[38,49] The normalized pinning force densities plotted versus the reduced field $b=B/B_{dep}$ can be described by the Kramer scaling $[F_p(B,T)\propto B_{dep}^2\sqrt{b}\,(1-b)^2]$ (Ref. 50) only in limited temperature regions. A convincing coincidence of the $F_p(B,T)$ data for all temperatures could not be achieved yet, which may be caused by significant differences in the peculiar vortex dynamics at higher fields for the different temperatures.

IV. CONCLUSIONS

We analyzed the resistive transitions by means of thermally assisted flux creep and found a linearly increasing activation energy with decreasing temperature depending on the magnetic field like $B^{-0.5}$ for current densities below 10^5 A/cm^2. These results are in full agreement with the model of Vinokur *et al.*[36] and describe the decay of resistivity within almost six orders of magnitude. Taking into account a mass anisotropy of 150, this model delivers even quantitatively correct results. Concerning the critical current density, the decay of j_c is still pronounced compared to $YBa_2Cu_3O_7$ for temperatures above 50 K, but the possible temperature and field regime for practical applications demanding at least $j_c > 10^4$ A/cm^2 is in these films significantly extended to higher temperatures as well as fields in comparison to prior data for epitaxial films. This improvement of critical current in the films, which was independent of the transport measurements also confirmed by magnetic relaxation experiments,[46] is related to a rigorous optimization of the film quality. There is evidence, that in these films with very low resistivity values and superior structural properties, the high j_c values are not related to the presence of "many defects" but to a suitable, low defect density.

ACKNOWLEDGMENTS

This work was financially supported by the Bundesministerium für Forschung und Technologie der Bundersrepublik Deutschland (Contract No. 13 N 5748 A) and by the Deutsche Forschungsgemeinschaft through SFB 252. We thank Dr. G. Jakob for helpful and clarifying discussions.

[1]R. Kleiner, F. Steinmeyer, G. Kunkel, and P. Müller, Phys. Rev. Lett. **68**, 2394 (1992).
[2]B. Aigner, B. Avenhaus, R. Kleiner, G. Kunkel, P. Pospischil, F. Steinmeyer, P. Müller, and K. Andres, IEEE Trans. Appl. Supercond. **3**, 2281 (1993).
[3]P. Schmitt, P. Kummeth, L. Schultz, and G. Saemann-Ischenko, Phys. Rev. Lett. **67**, 267 (1991).
[4]P. Wagner, H. Adrian, and C. Tomé Rosa, Physica C **195**, 258 (1992).
[5]P. Schmitt, L. Schultz, and G. Saemann-Ischenko, Physica C **168**, 475 (1990).
[6]G. Balestrino, M. Marinelli, E. Milani, M. Montuori, A. Paoletti, and P. Paroli, J. Appl. Phys. **72**, 191 (1992).
[7]J. N. Eckstein, I. Bozovic, M. E. Klausmeier-Brown, G. F. Virshup, and K. S. Ralls, Mater. Res. Bull. **27** (Aug. 1992), and references therein.
[8]C. J. van der Beek and P. H. Kes, Phys. Rev. B **43**, 13 032 (1991).
[9]G. Blatter, J. Rhyner, and V. M. Vinokur, Phys. Rev. B **43**, 7826 (1991).
[10]K. H. Müller, M. Nikolo, and R. Driver, Phys. Rev. B **43**, 7976 (1991).
[11]C. Gerber, D. Anselmetti, J. G. Bednorz, J. Mannhart, and D. G. Schlom, Nature (London) **350**, 279 (1991).
[12]P. Wagner, F. Hillmer, U. Frey, H. Adrian, T. Steinborn, L. Ranno, A. Elschner, I. Heyvaert, and Y. Bruynseraede, Physica C **215**, 123 (1993).
[13]R. Seemann, F. Hänisch, A. Sewing, R. L. Johnson, R. de Reus, and M. Nielsen, Physica C **199**, 112 (1992).
[14]The *ab* plane TEM images were taken by C. Traeholt at the University of Delft.
[15]X. F. Zhang, B. Kabius, K. Urban, P. Schmitt, L. Schultz, and G. Saemann-Ischenko, Physica C **194**, 253 (1992).
[16]H. Watanabe, B. Kabius, K. Urban, B. Roas, S. Klaumünzer, and G. Saemann-Ischenko, Physica C **179**, 75 (1991).
[17]B. Mayer, L. Alff, T. Träuble, R. Gross, P. Wagner, and H. Adrian, Appl. Phys. Lett. **63**, 996 (1993).
[18]P. Wagner, U. Frey, F. Hillmer, A. Hadish, G. Jakob, H. Adrian, T. Steinborn, L. Ranno, A. Elshner, I. Heyvaert, and Y. Bruynseraede, J. Superconduct. **7**, 217 (1994).
[19]The carrier density and mobility data were determined for the undoped films, data for $YBa_2Cu_3O_7$ can be found in an article by Speckmann *et al.*, Phys. Rev. B **47**, 15 185 (1993).
[20]A compilation of structural data for high-T_c materials is K. Yvon and M. Francios, Z. Phys. B **76**, 413 (1989).
[21]G. Blatter, V. B. Geshkenbein, and A. I. Larkin, Phys. Rev. Lett. **68**, 875 (1992).
[22]D. E. Farrell, S. Bonham, J. Foster, Y. C. Chang, P. Z. Jiang, K. G. Vandervoort, D. J. Lam, and V. G. Kogan, Phys. Rev. Lett. **63**, 782 (1989).
[23]H. Raffy, S. Labdi, O. Laborde, and P. Monceau, Phys. Rev. Lett. **66**, 2515 (1991).
[24]F. Steinmeyer, R. Kleiner, P. Müller, and K. Winzer (unpublished).
[25]E. Silva, R. Marcon, R. Fastampa, M. Giura, and S. Sarti, Physica C **214**, 175 (1993).
[26]T. T. M. Palstra, B. Batlogg, R. B. van Dover, L. F. Schneemeyer, and J. V. Wasczak, Phys. Rev. B **41**, 6621 (1990).
[27]E. Zeldov, N. M. Amer, G. Koren, and A. Gupta, Appl. Phys. Lett. **56**, 1700 (1990).
[28]H. Safar, P. L. Gammel, D. J. Bishop, D. B. Mitzi, and A. Kapitulnik, Phys. Rev. Lett. **68**, 2672 (1992).
[29]Ph. Seng, R. Gross, U. Baier, M. Rupp. D. Koelle, R. P. Huebener, P. Schmitt, G. Saemann-Ischenko, and L. Schultz, Physica C **192**, 403 (1992).
[30]T. T. M. Palstra, B. Batlogg, L. F. Schneemeyer, and J. V. Waszczak, Phys. Rev. B **43**, 3756 (1991).
[31]S.-T. Chui and Hong-ru Ma, J. Phys.: Condens. Matter **4**, L237 (1992).
[32]C. W. Hagen and R. Griessen, Phys. Rev. Lett. **62**, 2857 (1989).
[33]J. T. Kucera, T. P. Orlando, G. Virshup, and J. N. Eckstein, Phys. Rev. B **46**, 11 004 (1992).
[34]C. Tomé Rosa, G. Jakob, M. Pauslon, P. Wagner, A. Walkenhorst, M. Schmitt, and H. Adrian, Physica C **185-189**, 2175 (1991).
[35]V. Geshkenbein, A. Larkin, M. Feigel'man, and V. Vinokur, Physica C **162-164**, 239 (1989).
[36]V. M. Vinokur, M. V. Feigel'man, V. B. Geshkenbein, and A. I. Larkin, Phys. Rev. Lett. **65**, 259 (1990).
[37]C. Stölzel, M. Huth, and H. Adrian, Physica C **204**, 15 (1992).
[38]H. Yamasaki, K. Endo, S. Kosaka, M. Umeda, S. Yoshida, and K. Kajimura, Phys. Rev. Lett. **70**, 3331 (1993).
[39]G. Jakob, T. Hahn, C. Stölzel, C. Tomé Rosa, and H. Adrian, Europhys. Lett. **19**, 135 (1992).
[40]L. Antognazza, O. Brunner, L. Miéville, J.-M. Triscone, and Ø. Fischer, Physica C **185-189**, 2081 (1991).
[41]M. Schmitt, S. Freisem, A. Walkenhorst, G. Jakob, and H. Adrian (unpublished).
[42]D. H. Kim, K. E. Gray, R. T. Kampwirth, and D. M. McKay, Phys. Rev. B **42**, 6249 (1990).
[43]Y. Koike, T. Noji, Y. Saito, N. Kobayashi, T. Nakanomyo, T. Goto, and T. Fukase, Sci. Rep. Res. Inst. Tohoku Univ. Ser. A **37**, 151 (1992).
[44]B. vom Hedt, K. Westerholt, and H. Bach (unpublished).
[45]P. Schmitt, Ph.D. thesis, University Erlangen-Nürnberg, 1992 (unpublished).
[46]V. V. Metlushko, G. Güntherodt, P. Wagner, H. Adrian, I. N. Goncharov, V. V. Moshchalkov, and Y. Bruynseraede, Appl. Phys. Lett. **63**, 2821 (1993).
[47]G. Jakob, M. Schmitt, Th. Kluge, C. Tomé Rosa, P. Wagner, Th. Hahn, and H. Adrian, Phys. Rev. B **47**, 12 099 (1993).
[48]M. Speckmann, Th. Kluge, C. Tomé Rosa, Th. Becherer, and H. Adrian, Phys. Rev. B **47**, 15 185 (1993).
[49]H. Yamasaki, K. Endo, S. Kosaka, M. Umeda, S. Yoshida, and K. Kajimura (unpublished).
[50]E. J. Kramer, J. Appl. Phys. **44**, 1360 (1973).